OMTO, Volume *21*

Supplemental information

Secretion of bispecific protein of anti-PD-1 fused with TGF-β trap enhances antitumor efficacy of CAR-T cell therapy

Xianhui Chen, Shuai Yang, Si Li, Yun Qu, Hsuan-Yao Wang, Jiangyue Liu, Zachary S. Dunn, Gunce E. Cinay, Melanie A. MacMullan, Fangheng Hu, Xiaoyang Zhang, and Pin Wang

Supplementary Materials

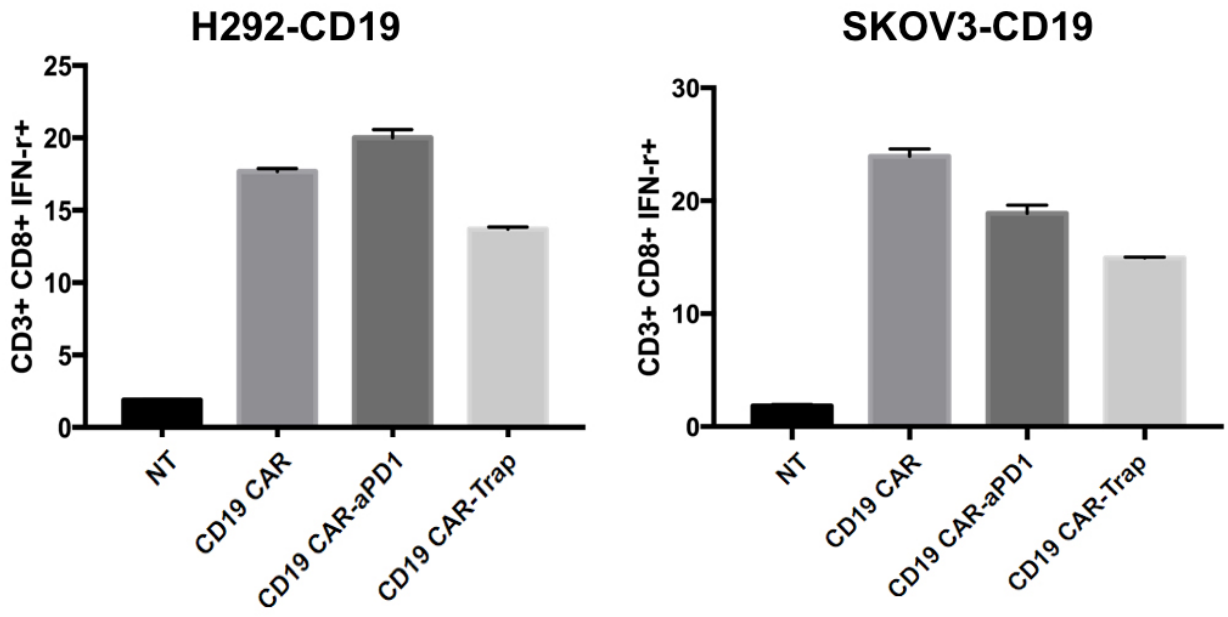

Supplementary Fig. S1. IFN-γ expression was measured by flow cytometry after CAR T cells were co-cultured with H292-CD19 cells and SKOV3-CD19 cells for 16 hours in the presence of protein transport inhibitor Brefeldin A. The percentage of IFN-γ+ T cells over total CD8+ T cells was shown in bar graphs (n=3, mean ± SD; ns, not significant; **P < 0.01).

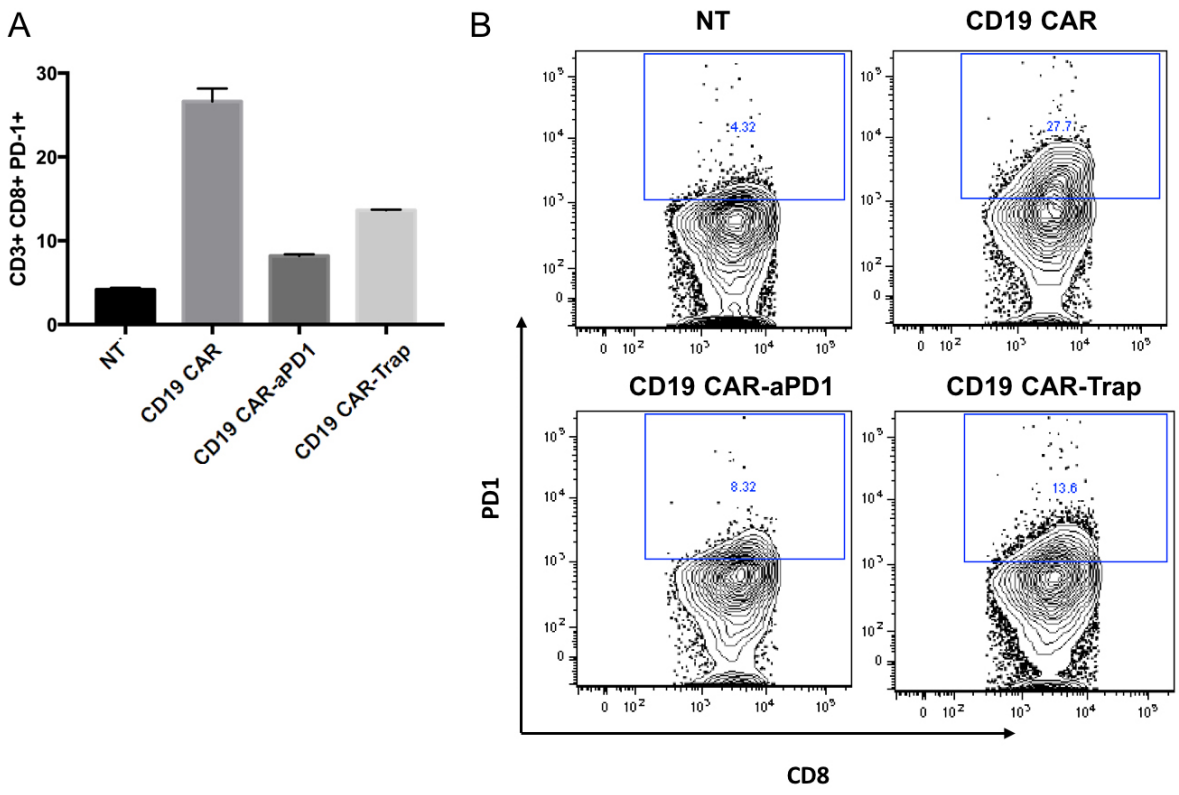

Supplementary Fig. S2. CAR-T cells were co-cultured with H292-CD19 cells for 24 hours. **(A)** The percentages of PD-1+CD8+ T cells over total CD8+ T cells were shown in bar graphs. (n=3, mean ± SD; ***P < 0.001). **(B)** CD3+ T cells were shown in each panel. PD-1+CD8+ T cells were gated, and their percentage over total CD3+ T cells was shown in each scatter plot.

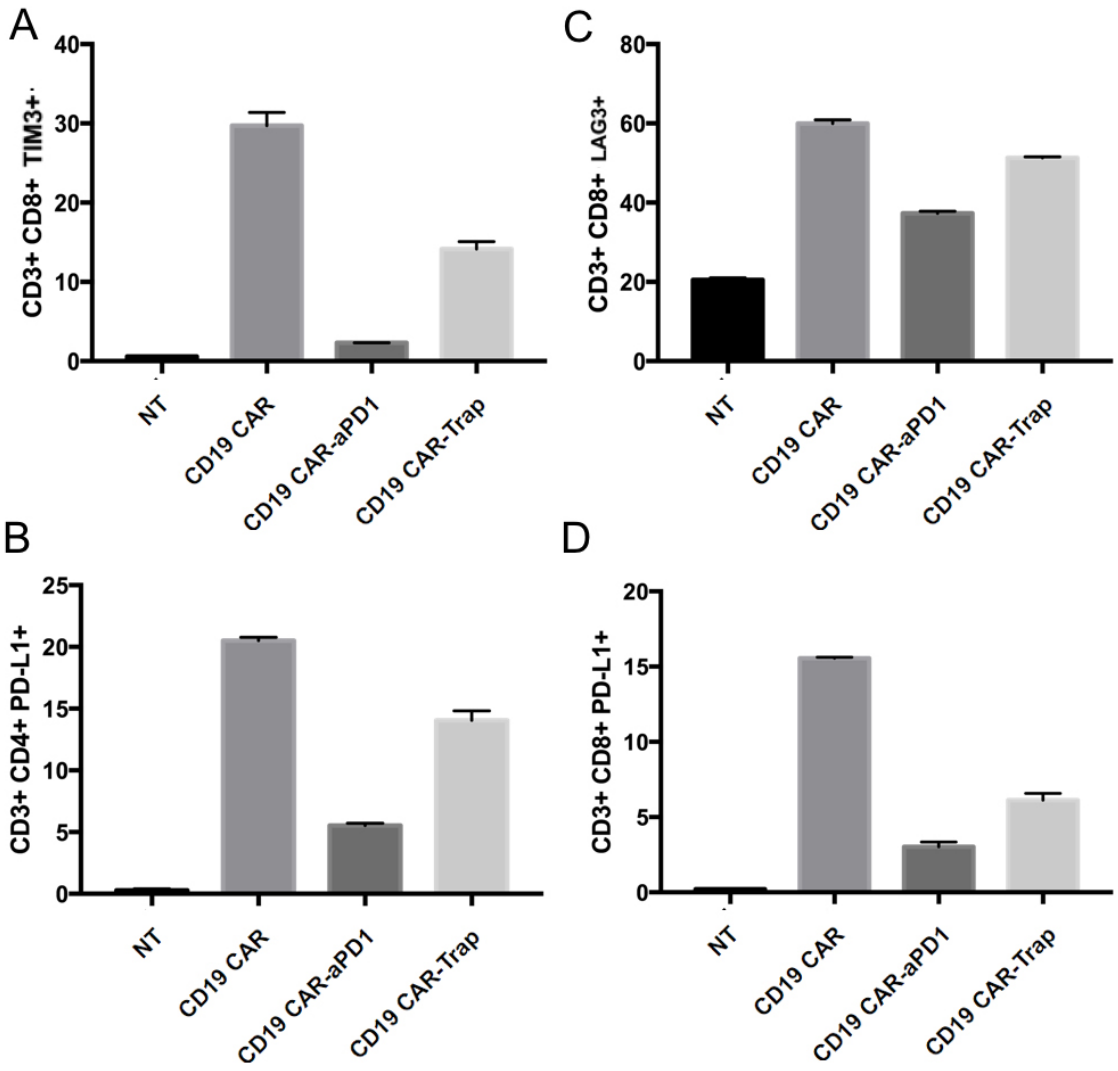

Supplementary Fig. S3. CAR T cells were co-cultured with H292-CD19 cells for 24 hours. **(A, B)** TIM3 expression and LAG3 expression were measured by flow cytometry. The percentages of $TIM3^+CD8^+$ and $LAG3^+CD8^+$ T cells over total $CD8^+$ T cells were shown in bar graphs. (n=3, mean ± SD; ns, not significant, **P < 0.01). **(C, D)** PD-L1 expression was measured by flow cytometry. The percentages of $PD\text{-}L1^+CD4^+$ and $PD\text{-}L1^+CD8^+$ over total $CD4^+$ and $CD8^+$ T cells were shown in bar graphs. (n=3, mean ± SD; *P < 0.05; **P < 0.01).

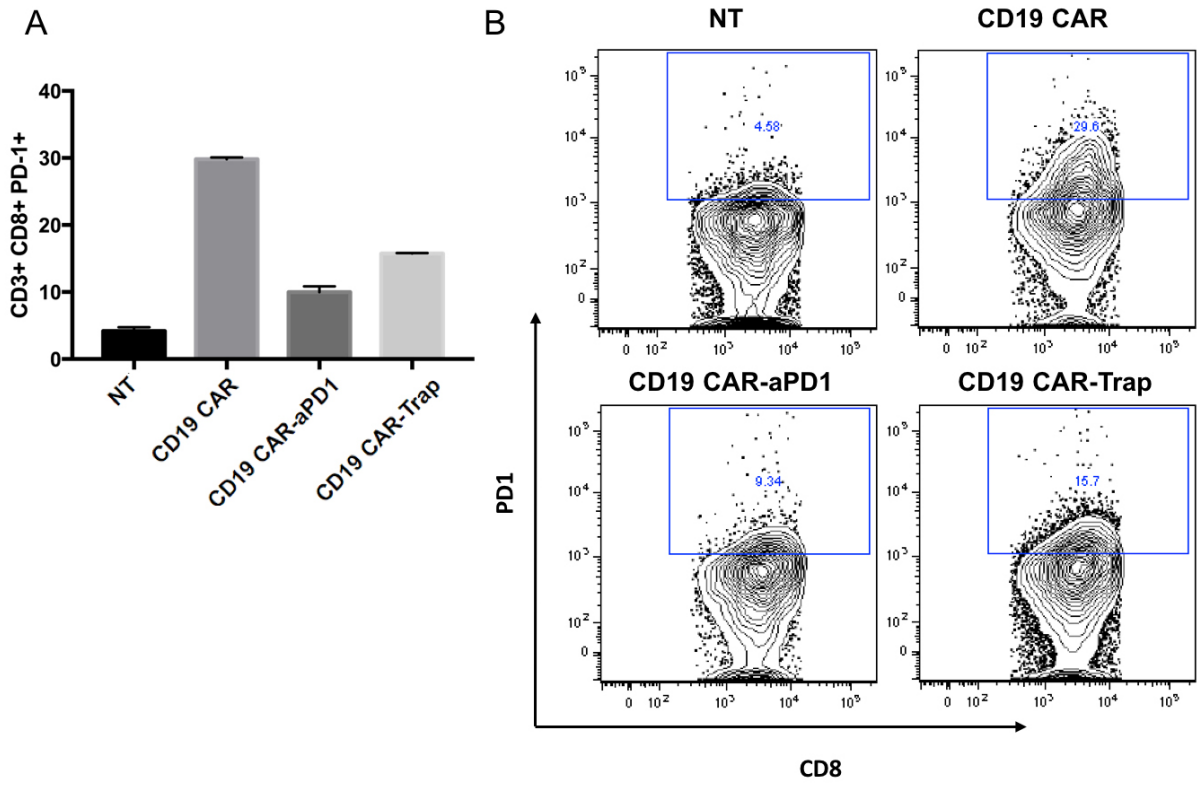

Supplementary Fig. S4. CAR-T cells were co-cultured with SKOV3-CD19 cells for 24 hours. **(A)** The percentages of PD-1^{+}CD8^{+} T cells over total CD8^{+} T cells were shown in bar graphs. (n=3, mean ± SD; ***P < 0.001). **(B)** CD3^{+} T cells were shown in each panel. PD-1^{+}CD8^{+} T cells were gated, and their percentage over total CD3^{+} T cells was shown in each scatter plot.

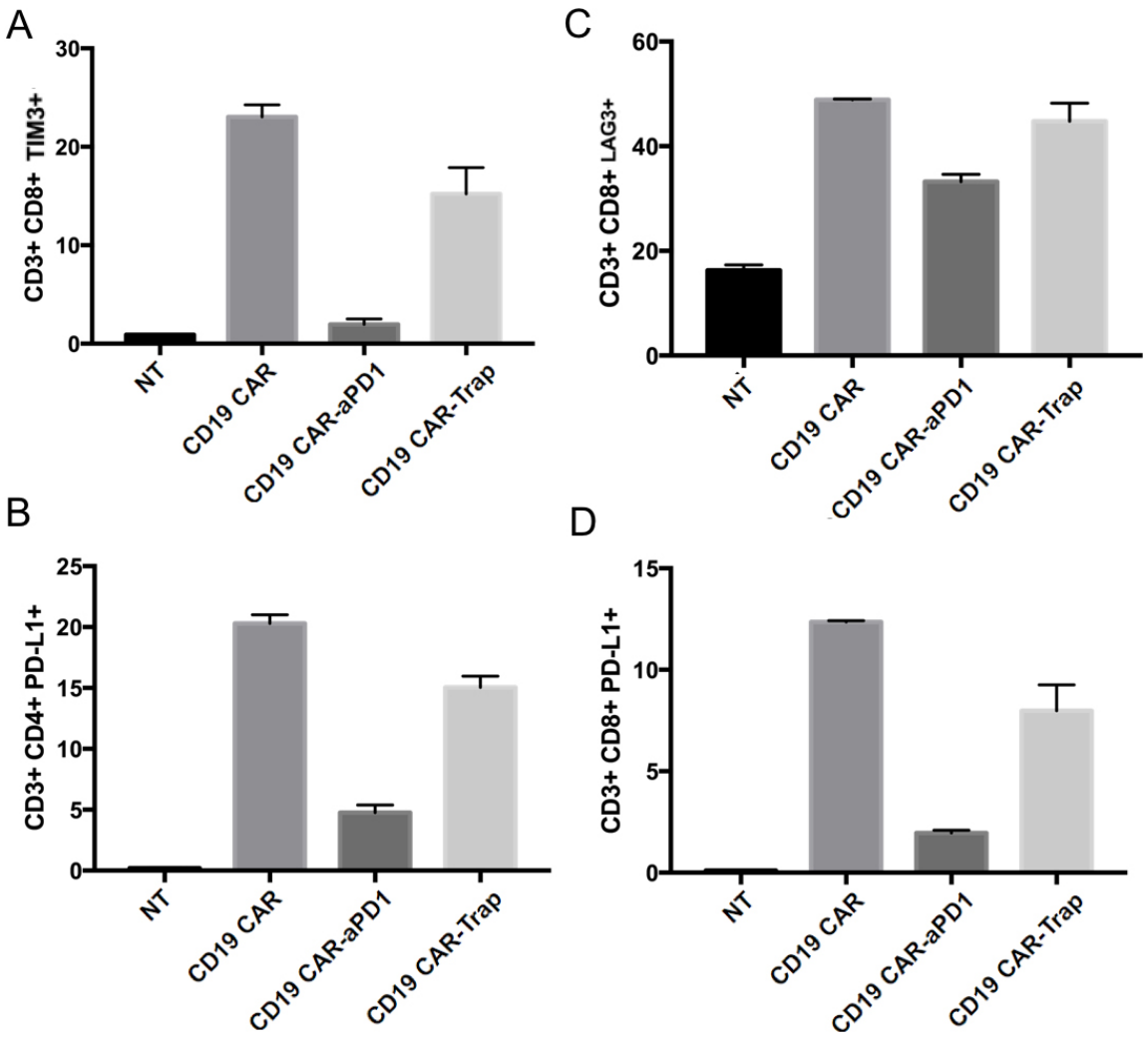

Supplementary Fig. S5. CAR T cells were co-cultured with SKOV3-CD19 cells for 24 hours. **(A, B)** TIM3 expression and LAG3 expression were measured by flow cytometry. The percentages of $TIM3^+CD8^+$ and $LAG3^+CD8^+$ T cells over total $CD8^+$ T cells were shown in bar graphs. (n=3, mean ± SD; ns, not significant, $^{**}P < 0.01$). **(C, D)** PD-L1 expression was measured by flow cytometry. The percentages of $PD\text{-}L1^+CD4^+$ and $PD\text{-}L1^+CD8^+$ T cells over total $CD4^+$ and $CD8^+$ T cells were shown in bar graphs. (n=3, mean ± SD; $^*P < 0.05$; $^{**}P < 0.01$).

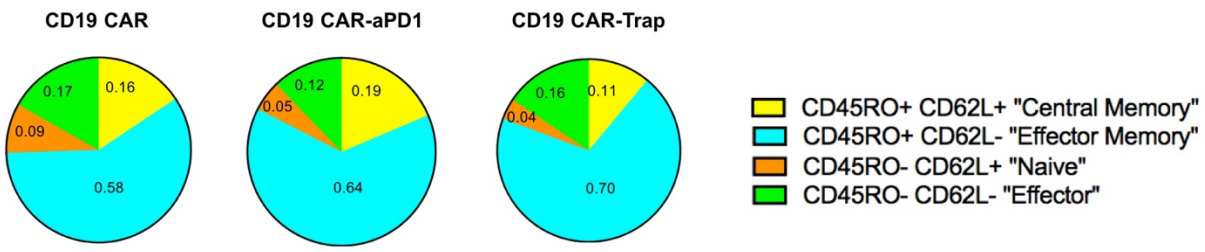

Supplementary Fig. S6. Tumor samples collected from CD19 CAR, CD19 CAR-αPD1 or CD19 CAR-Trap T cell-treated groups on day 12 post-treatment were analyzed for memory status. Samples were stained for human CD45RO and CD62L and then measured by flow cytometry. The average percentages of naïve T cells, effector memory T cells, central memory T cells and effector T cells were shown in pie graphs.

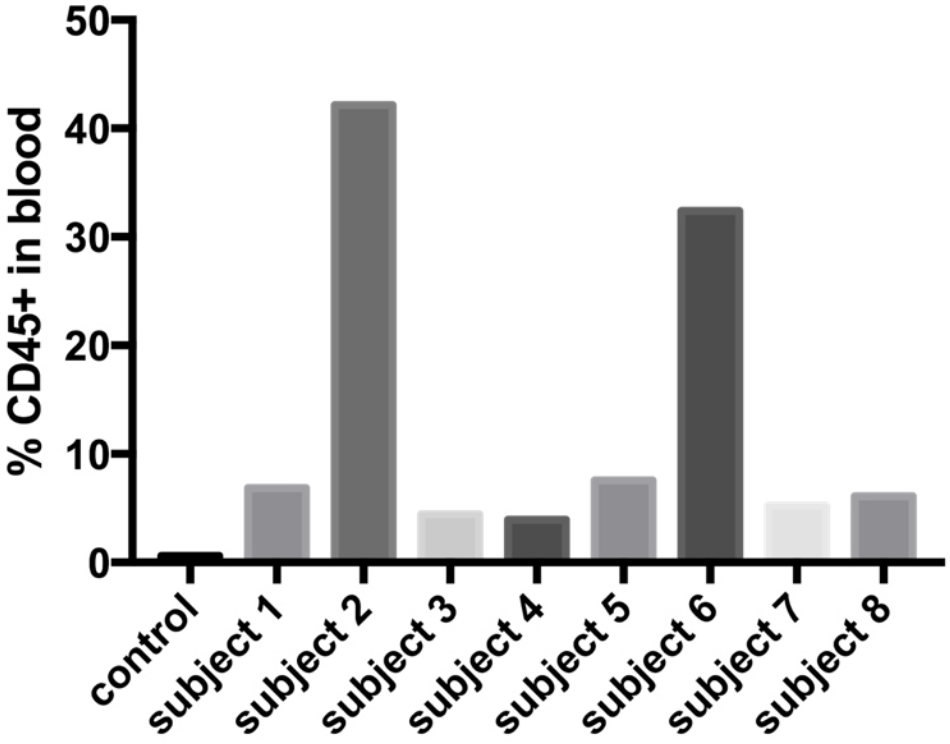

Supplementary Fig. S7. Eight mice of CD19 CAR-Trap group were bled on day 61 post-treatment of 4 x 10^6 CAR-T cells. The blood samples were lysed to remove red blood cells and then processed for T cell analysis. The percentages of T cells in blood of each mouse were shown in bar graphs.